Green Behavior Diffusion with Positive and Negative Information in Time-varying Multiplex Networks

Xianli Sun, Linghua Zhang, Qiqing Zhai, and Peng Zheng

***Abstract*—How to comprehend the relationship between information spreading and individual behavior adoption is an essential problem in complex networks. To this end, a novel two-layer model to depict the diffusion of green behavior under the impact of positive and negative information is proposed. Positive information motivates people to adopt green behavior, while negative information reduces the adoption of green behavior. In the model, the physical contact layer describes the green behavior diffusion, and the information layer describes the positive and negative information spreading. Moreover, the social interactions of individuals in two layers change with time and are illustrated by an activity-driven model. Then, we develop the probability transition equations and derive the green behavior threshold. Next, experiments are carried out to confirm the preciseness and theoretical predictions of the new model. It reveals that the prevalence of green behavior can be promoted by restraining the negative information transmission rate and recovery rate of the green nodes while facilitating the positive information transmission rate and green behavior transmission rate. Additionally, reducing the positive information recovery rate and the recovery rate of the green nodes, and increasing the rates of forgetting negative information are beneficial for encouraging the outbreak of green behavior. Furthermore, in the physical contact layer, higher contact capacity and greater activity heterogeneity significantly facilitate green behavior spreading. In the information layer, smaller contact capacity and weaker activity heterogeneity promote diffusion when negative information dominates, whereas larger contact capacity and stronger activity heterogeneity are beneficial when positive information prevails.**

***Index Terms*—Green behavior diffusion, multiplex network, negative information, positive information, time-varying.**

Manuscript received April 16, 2024; revised September 5, 2024; approved for publication by Kim, Hyoil Division 3 Editor, October 5, 2024.

This work was supported by the National Natural Science Foundation of China under Grant 62371253 and the Graduate Scientific Research and Innovation Program of Jiangsu Province under Grant KYCX24_1179. *(Corresponding author: Linghua Zhang.)*

X. Sun is with the School of Telecommunications and Information Engineering, Nanjing University of Posts and Telecommunications, Nanjing 210003, China, email: 1151176147@qq.com.

L. Zhang is with the School of Telecommunications and Information Engineering, Nanjing University of Posts and Telecommunications, Nanjing 210003, China and with the Jiangsu Engineering Research Center of Communication and Network Technology, Nanjing University of Posts and Telecommunication, Nanjing, 210003, China, email: zhanglh@njupt.edu.cn.

Q. Zhai is with the School of Science, Nanjing University of Posts and Telecommunication, Nanjing, 210023, China, email: qiqingzhai@163.com.

P. Zheng is with the School of Computer Science, Nanjing University of Posts and Telecommunication, Nanjing, 210023, China, email: 1403404665@qq.com.

L. Zhang is the corresponding author.

Digital Object Identifier: 10.23919/JCN.2024.00.

I. Introduction

A. Background and Motivation

In the era of global warming, reducing carbon emissions has become an essential issue, capturing worldwide attention [1]. An increasing number of individuals have become conscious of the perilous state of our environment and energy sources, and are strongly advocating green behavior. Green behavior is the activities of individuals or social organizations who embrace the world's green principles, such as opting for recycling materials, public transportation, efficiently utilizing energy, and safeguarding the species and living environment [2]. Given the critical role that green behavior plays in mitigating environmental degradation, it is essential to understand how these behaviors spread through populations to effectively promote sustainable practices.

To understand how green behavior spreads, it is essential to consider the context of complex networks, which are ubiquitous in various systems such as cells, the human brain, ecosystems, and the Internet [3]. Based on the theory of complex networks, researchers can more accurately model the diffusion process, such as information diffusion [4], green behavior diffusion [2], and rumor diffusion [5]. Since green behavior diffusion is often considered to be similar to epidemic diffusion, many researchers simulate the diffusion dynamics of green behavior based on the classical epidemic spreading model [6]. However, real-world systems are frequently associated with each other, complex systems may be made up of several interacting sub-systems [7]. For instance, the power grids frequently rely on the communication systems to transmit the controlling signals, while communication systems typically depend on power grids for their operation [8]. Additionally, offline people persuade their friends to adopt one thing (opinion, product, or service) through word-of-mouth, while online information cascades through social networks can influence offline behavior [9]. As a result, investigating the dynamics and structure on top of multi-layer networks is currently a hot topic in the study of complex systems.

As network technology has advanced, online social networks have evolved into a momentous stage for people to communicate, exchange information, and share files [10]. With the growing concern about environmental issues, information related to green behavior propagating through online social networks, may wield considerable influence on the adoption of green behavior [11]. Once individuals acquire information about green behavior from online social networks, they are

1229-2470/24/$10.00 © 2024 KICS

likely to adopt corresponding green behavior to protect the environment [12]. Actually, plenty of connections among actual individuals take place at different levels and exert mutual effects. Hence, a two-layer network should be considered to depict the dynamic interplay between green behavior spreading and information diffusion [6].

Nowadays, multiplex networks have gained widespread to model the dynamic propagation process among individuals at different layers [13]. In a multiplex network, there are two layers: the information layer and the physical contact layer. These layers interact and influence each other, providing a more comprehensive framework to study the spread of green behavior and the diffusion of information.

Even though the previous models properly depict the relationship between information diffusion and green behavior, the spread of green behavior reveals some novel characteristics. Many works focused on the impact of a single type of information on green behavior, for example, all people are likely to receive messages that support green behavior. In practice, individuals may exhibit different attitudes toward green behavior, and individuals' behavior may display significant heterogeneity [14]. Specifically, when green behaviors propagate in the physical contact layer, some negative information regarding green behavior emerges, which can potentially discourage individuals from adopting green behavior [15]. For example, when it comes to commutes, some people in remote areas contend that car-dependent lifestyles normalize their recreation, work, and residence, and green behavior may reduce the convenience of people's lives [16]. Moreover, with regard to the purchase of green goods, some people think that the green feature is accompanied by premium pricing which leads to them giving up green goods [17]. In reality, customers will not compromise their requirements or desires for the sake of environmental sustainability. Conversely, in order to reduce carbon emissions and preserve energy, some people actively promote and practice green behavior. Hence, there are typically two forms of information about green behavior that propagate simultaneously on social networks: 1) positive information; and 2) negative information. People can be influenced by different information about green behavior in online social networks to decide whether they adopt green behavior. Therefore, it is imperative to delve into the effect of various information on the dissemination of green behavior.

Additionally, many studies focus on the spreading model in static networks. Static connections and interactions are approximations, representing time-aggregated versions of actual interactions [18]. In other words, these models can be characterized as connectivity models, where the connections between individuals are long-lasting elements [19]. This approach completely ignores the time-varying nature of connectivity patterns. Actually, with the prevalence of diverse social networks, interactions among individuals are often rapidly changing and occur within a very short timeframe, such as mobile calls between individuals or the rapid diffusion of information through email [20]. To more accurately understand spreading dynamics in the real world, it is essential to consider the time-dependent interactions between network layers [21]. Therefore, in this paper, we consider the time-varying multiplex networks to describe the dynamic interplay between the information layer and the physical contact layer.

B. Main Contributions

For the sake of getting over the restrictions mentioned above, we develop a new dynamics model called $UA_1A_2U - SGS$ model, which can precisely depict the process of green behavior propagation. Moreover, we consider time-varying interactions in networks to make the model more grounded in reality. This paper's main contributions are summarised below.

1) $UA_1A_2U - SGS$ *model*: Considering the educational background, the accumulation of knowledge, income, region, etc., individuals have different levels of perceptions, which leads to different attitudes toward green behaviors. Specifically, there exist typically two forms of information about green behavior that propagate in social networks: Positive information and negative information. People can be simultaneously influenced by two types of information about green behavior in online social networks to decide whether they adopt green behavior. Then, we propose the $UA_1A_2U - SGS$ model for analyzing the interaction between green behavior and information, which utilizes two-layered multiplex networks.
2) *Time-varying multiplex networks*: Considering interactions among individuals frequently change over time in real-world scenarios, time-varying networks can more accurately capture the fundamental characteristics of complex systems [22]. Thus, we adopt the activity-driven network to describe the physical contact layer and information layer, making both layers time-varying.
3) *Green behavior threshold*: Predicting the threshold for the propagation of green behavior holds profound significance in safeguarding the environment. Thus, we calculate the green behavior threshold of the UA_1A_2U-SGS model using the microscopic Markov chain.

C. Outline

The paper is organized as follows. We review the related works in Section II. We develop a novel dynamics model of the green behavior and information propagation in multiplex networks in Section III. In Section IV, we compute the green behavior threshold by the microscopic Markov chain. The extensive simulations are conducted in Section V. Lastly, the conclusions of this paper are clarified in Section VI.

II. Related Work

A. The Development of Green Behavior Model

The topic of green sustainable development has grown in prominence as a significant human concern. Understanding the dynamics of how green behavior spreads can significantly enhance the effectiveness of interventions aimed at promoting sustainable practices.

In single-layer networks, the green behavior spreading model typically involves analyzing the factors that influence

green behavior, such as environmental education [23], energy price [24], environmental activist behavior [25], and transportation [26]. Li *et al.* [27] combined the game theory with green behavior, and found that people tend to prioritize adopting green behavior when they display a lower activity rate or higher connectivity. Wang *et al.* [28] investigated the impact of information regarding green attributes and green certification on consumer perceptions. Geng *et al.* [15] proposed a three-color theoretical model, exploring motivation and behavior in a two-dimensional context. Kyoi *et al.* [29] developed a dynamic model in social networks to depict the spread of pro-environmental behaviors and identify promising approaches for supporting them.

Moving beyond single-layer networks, researchers have explored the diffusion of green behavior in multiplex networks. Multiplex networks provide a more realistic representation of social systems, capturing the complexity of how individuals interact across various contexts such as family, work, and social circles. The advent of online social networks has witnessed an unparalleled surge in their adoption, profoundly transforming the landscape of interpersonal communication and prompting extensive research into their impacts on offline user behavior [30], such as green behavior [31], voting [32], health behavior [33], and epidemic spreading [34]. Therefore, many studies focused on the coupled diffusion of information on online social networks and green behavior in the physical contact layer. Gao *et al.* [35] investigated green behavior and knowledge propagation in multiplex networks and found that government policies are critical to green behavior diffusion. According to the Microscopic Markov Chain Approach, Li *et al.* [11] investigated the influence of information propagation on green behavior spreading in multiplex networks. Li *et al.* [31] investigated the effects of negative information diffusion on green behaviors employing the HGBS model. Yin *et al.* [2] developed a dynamic model to depict that green behavior spreading is not only related to green information but also influenced by changes in social relationships.

B. The Development of the Time-varying Multiplex Networks

Temporal networks allow information and green behavior propagation along links only when they exist in time, and this leads to considerable influences on propagation efficiency [36]. Currently, the activity-driven model is one of the main time-dependent systems, which highlights the structure's response to its dynamics. The activity-driven model is simple in its basic form and produces a nontrivial temporal structure that affects how dynamical processes develop [37]. Due to its simplicity, the initial activity-driven model is unable to reproduce some common characteristics of social networks, such as memory effects, and assortative mixing [38]. Thanks to these reasons, modifications to the initial model have been implemented and investigated [39]. Chai *et al.* [40] introduced activity-driven networks to characterize realistic temporal networks, and the node-based SIRS model was used to depict the dissemination dynamics from a microcosmic aspect. Pozzana *et al.* [41] studied SIS spreading processes using a recently developed extension of the activity-driven modeling framework.

Based on the activity-driven model, scholars have extended their work to multiplex networks. Guo *et al.* [42] considered that the layer of information is an activity-driven network, whereas the layer of physical contact is a static network. Li *et al.* [43] regarded information spreading network as a static network, while physical contact network is time-varying. Yang *et al.* [18] depicted information and epidemic diffusion in an activity-driven multiplex network. Huang *et al.* [44] analyzed the dynamic model of epidemic propagation and resource dissemination in time-varying multiplex networks. Unfortunately, research on green behavior in time-varying multiplex networks is scarce. Therefore, we focus on the diffusion of green behavior in time-varying multiplex networks.

III. Coupled Dynamic Model of Information Spreading and Green Behavior Diffusion

A. Time-varying Multiplex Networks

Given that human behavior is generally transmitted through face-to-face interactions, those who live or work in close proximity often have a substantial influence on your behavior. Thus, green behavior propagates through a physical contact network, wherein the connections represent relationships with individuals you encounter daily, such as colleagues, neighbors, and family members. Moreover, messages about green behavior diffuse through an information network, where the connections represent relationships with individuals with whom you share information. Once individuals acquire information about green behavior from an information network, they are likely to adopt corresponding green behavior to protect the environment. Therefore, in addition to regular physical contact, this network should also encompass connections established through digital communication channels [11].

To depict the dynamic interaction between the dissemination of green behavior and information, two-layered multiplex networks are utilized. The lower layer is the physical contact network P, illustrating the spread of green behavior, while the upper layer is the information network V, such as Facebook or WeChat, focusing on the dissemination of information related to green behavior. Specifically, in two-layered networks, the mapping relation between associated individuals is one-to-one, which means each individual exists concurrently in the information layer and the physical contact layer [45]. Additionally, each edge in the two-layered network is assumed to be unweighted and undirected.

We employ the activity-driven model to create each layer of the networks. Fig. 1 displays the procedures involved in building the time-varying multiplex network. The network consists of N nodes, each with a fixed activity level that determines the chance of the node being activated and establishing new connections with other nodes. Specifically, in the information layer V, the activity level of the node i is $a_i = \eta_v x_i$, and in the physical contact layer P is $b_i = \eta_p y_i$. Parameters of x_i and y_i represent the activity potentials following power-law distributions $F_v(x) \propto x^{-\gamma_v}$ and $F_p(x) \propto y^{-\gamma_p}$, respectively [46]. Parameters of η_v and η_p are the rescaling factors. Moreover,

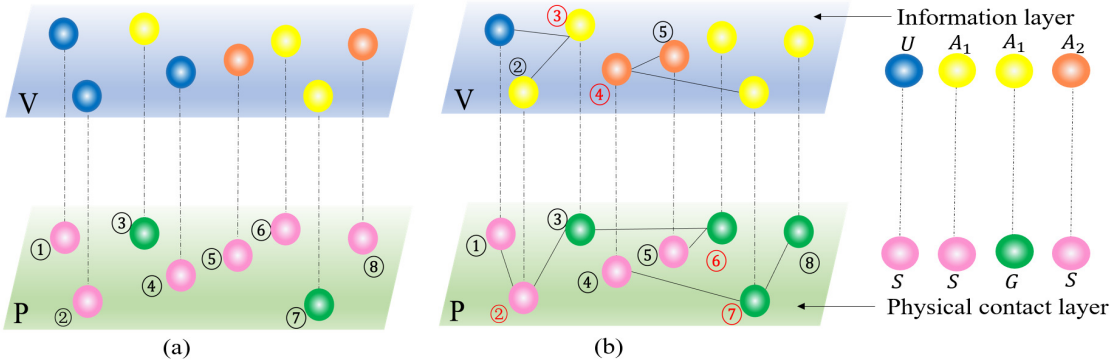

Fig. 1. Schematic diagram of the coupled UA_1A_2U-SGS model in time-varying multiplex networks. The upper layer is the information layer V representing the diffusion of positive and negative information, where nodes have three possible states: U (unaware of green information); A_1 (aware of positive green information); and A_2 (aware of negative green information). The lower one is the physical contact layer P describing the green behavior propagation, where nodes also have two possible states: susceptible (S) and green (G). The dotted lines connecting two layers denote the one-to-one relationship between individuals. Each node has its corresponding activity level. (a) Firstly, some isolated nodes in the two layers with different activity levels. In the physical contact layer, nodes 3 and 7 are randomly chosen as green nodes. Thus, the two individuals in the information layer are in the state of A_1, and the others are in the state of US, A_1S and A_2S. (b) Secondly, according to the activity levels of nodes, an instantaneous network is generated that nodes 2, 6, and 7 in the physical contact layer and nodes 3, and 4 in the information layer are activated, as shown by a red number near each node. Each active node generates 2 inks to randomly connect other nodes. For example, node 2 receives information from node 3 in the layer V, and node 4 receives information from node 5 in the layer V. In the layer P, node 8 is infected by node 7 and turns to the state of A_1 in the layer V. All connections are eliminated at the subsequent step and the step of (b) is repeated until the diffusion has either ceased or achieved a stationary state in both layers.

parameters of γ_v and γ_p refer to activity exponents of the upper and lower layers, respectively [47].

Definition 1: (Activity-driven network) Based on the configurations, the generative steps of the activity-driven network (ADN) are as follows.

- At time t, each layer is comprised of N nodes that are separated from each other, and there exists a one-to-one relationship between nodes in two layers.
- The node i becomes active with a probability of $a_i\Delta t$ ($b_i\Delta t$), and produces m_v (m_p) connections to other nodes that are chosen at random.
- At the next time step $t+\Delta t$, we remove all connections and repeat the first and second phases until the diffusion reaches a stationary state or is terminated in both layers.

B. The Description of the UA_1A_2U-SGS Model

In the upper layer, the UA_1A_2U model is proposed to depict the green information diffusion. Nodes in this layer are divided into three groups: U (unaware of green information); A_1 (aware of positive green information); and A_2 (aware of negative green information). People in state A_1 receive positive messages and agree on the importance of green behavior which contributes to adopting green behavior. Yet, people in state A_2 receiving negative information, such as the inconvenience of transport [15], and relatively high expenses of green consumption [48], are not conducive to adopting green behavior. People in states A_1 and A_2 will spread information about the positive and negative information of green behavior to their neighbors in multiplex networks, respectively. In addition, individuals have not received any information on green behavior in the state U, but can get it by communicating with aware neighbors.

In the lower layer, the SGS green behavior model is employed to represent the green behavior diffusion. Then, individuals are divided into two groups: 1) S (susceptible) and 2) G (green). On the one hand, the green node encourages the susceptible individuals to follow the green behavior, and on the other hand, they can abandon the green behavior due to price, income, or other reasons and return to the S state. Susceptible nodes have the potential to adopt the green behavior by contacting a green individual.

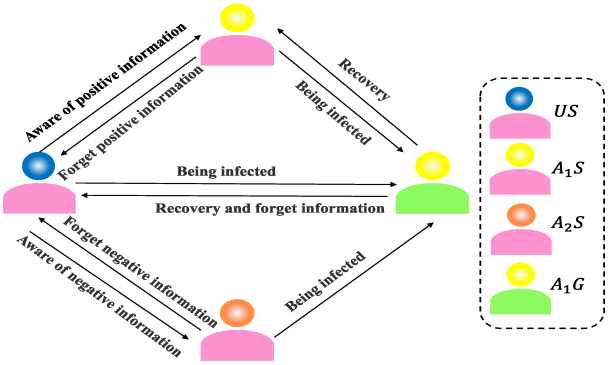

Fig. 2. The possible state transition for the UA_1A_2U-SGS model. The US nodes will receive the corresponding information disseminated by the spreaders of positive or negative information and turn to the state of A_1S or A_2S. Moreover, nodes in states A_1S and A_2S may change into the state US because of forgetting or losing interest in the green information. The US, A_1S and A_2S nodes may be infected by the green nodes and transfer to the state of A_1G. Besides, green nodes will also give up practicing green behavior and return to the state of US, A_1S or A_2S.

Based on the coupling of information diffusion and green behavior propagation, there exist six states: US, UG, A_1S, A_1G, A_2S, and A_2G. Moreover, once individuals are in the green state, they must be aware of the information about green behavior and thus UG cannot be included in the model. Additionally, if nodes are in the green state, they will transmit positive information to encourage neighbors to follow green behavior, and thus A_2G is excluded from the

model. Therefore, we only consider four potential states in multiplex networks: 1) A_1S (who is susceptible and aware of positive information); 2) A_2S (who is susceptible and aware of negative information); 3) US (who is susceptible and unaware of any information); and 4) A_1G (who is green and aware of positive information). Additionally, we assume that if an individual accepts a specific type of information, they are unlikely to accept any other information. Fig. 2 displays the diagram of the potential state transition for the $UA_1A_2U - SGS$ model.

According to the above description of different states, the propagation rules for the $UA_1A_2U - SGS$ model can be summarized as follows.

- The US nodes will receive the corresponding information disseminated by the spreaders of positive or negative information at rates λ_1 and λ_2, respectively.
- Nodes in states A_1S and A_2S may return to the state US because of forgetting or losing interest in the green information at the recovery rate δ_1 and δ_2, respectively. Furthermore, green nodes do not forget the positive information about green behavior before they give up practicing green behavior.
- When susceptible nodes come into contact with green nodes, their behaviors receive the influence of a green neighbor and are infected to be green nodes. The green nodes can propagate green behavior to their susceptible neighbors with probability β.
- Besides, green nodes will also give up practicing green behavior with a recovery rate μ.

Parameters γ_1 and γ_2 $\left(1 \leq \gamma_1 \leq 1/\beta^U, 0 \leq \gamma_2 \leq 1\right)$ are used to control the impact of positive nodes and negative nodes in the information layer on the physical contact layer, respectively. Compared with unaware nodes, aware nodes whose state is A_1S are more inclined to act in an ecologically beneficial way, and nodes whose state is A_2S are skeptical of green behavior [49]. Thus, we use γ_1 and γ_2 to distinguish the adoption rate among A_1S, A_2S, and US nodes. If an individual is in the state of US, its adoption rate of green behavior is β^U, while adoption rates of A_1S and A_2S nodes are represented by $\beta^{A_1} = \gamma_1\beta^U$ and $\beta^{A_2} = \gamma_2\beta^U$. When the values of γ_1 and γ_2 are bigger, the nodes are more likely to practice green behavior. In particular, when $\gamma_1 = 1$ and $\gamma_2 = 1$, interactions between two layers disappear, and the configuration is equal to executing the dynamic diffusion in the single-layer network.

IV. Theoretical Analysis based on the Microscopic Markov Chain Approach

Based on the microscopic Markov chain (MMC) approach [50], the green behavior threshold β_c is derived. In our model, there exist four possible states: 1) A_1S; 2) A_2S; 3) US; and 4) A_1G. At time t, the possibility that a node i is in each of the four states can be defined as $P_i^{A_1S}(t)$, $P_i^{A_2S}(t)$, $P_i^{US}(t)$, and $P_i^{A_1G}(t)$, respectively. Moreover, the normalized condition $P_i^{A_1S}(t) + P_i^{A_2S}(t) + P_i^{A_1G}(t) + P_i^{US}(t) = 1$ should be satisfied. The notations of all symbols are shown in Table I.

In the upper layer, at time t, the probability of the node i is not informed of positive or negative information by $r_i^{A_1}(t)$ and $r_i^{A_2}(t)$, respectively. Additionally, if the node is not informed of the positive or negative information, at the time step t, the possibility that the node will not affected by neighbors is defined as $q_i^U(t)$. Similarly, the possibility that the node i in the physical layer in A_1 or A_2 is not affected by its green neighbors is expressed as $q_i^{A_1}(t)$ and $q_i^{A_2}(t)$, respectively. The expressions of $r_i^{A_1}(t)$ and $r_i^{A_2}(t)$ are described as follows:

$$r_i^{A_1}(t) = \prod_j \left[1 - \lambda_1 \frac{m_v}{N} P_j^{A_1}(t)(a_i + a_j)\right], \tag{1}$$

$$r_i^{A_2}(t) = \prod_j \left[1 - \lambda_2 \frac{m_v}{N} P_j^{A_2}(t)(a_i + a_j)\right], \tag{2}$$

where $P_j^{A_1}(t) = P_j^{A_1S}(t) + P_j^{A_1G}(t)$ and $P_j^{A_2}(t) = P_j^{A_2S}(t)$. According to the theory of the activity-driven model [21], the expression for $m_v P_j^{A_1}(t)(a_i + a_j)/N$ is the possibility that i and j in the information layer are neighbors, where the first part $m_v a_i P_j^{A_1}(t)/N$ represents the active node i that establishes a connection with node j that is in the state A_1 and the other part $m_v a_j P_j^{A_1}(t)/N$ represents the individual i receiving a connection from the active individual j in the state A_1. The expression for $m_v P_j^{A_2}(t)(a_i + a_j)/N$ represents the possibility that the node i and j in the state A_2 are neighbors in the information layer. Similarly, the expressions of $q_i^U(t)$, $q_i^{A_1}(t)$, and $q_i^{A_2}(t)$ are described as follows:

$$q_i^{A_1}(t) = \prod_j \left[1 - \beta^{A_1} \frac{m_p}{N} P_j^{A_1G}(t)(b_i + b_j)\right], \tag{3}$$

$$q_i^{A_2}(t) = \prod_j \left[1 - \beta^{A_2} \frac{m_p}{N} P_j^{A_1G}(t)(b_i + b_j)\right], \tag{4}$$

$$q_i^{U}(t) = \prod_j \left[1 - \beta^{U} \frac{m_p}{N} P_j^{A_1G}(t)(b_i + b_j)\right], \tag{5}$$

where $m_p P_j^{A_1G}(t)(b_i + b_j)/N$ is the possibility that i and j in the physical contact layer which is in the A_1G state are neighbors. Based on the above definitions, Fig. 3 shows the probability trees of different states in multiplex networks.

The features of the asymmetrically interacting diffusion dynamics in time-varying multiplex networks suggest that the microscopic Markov chain approach should be employed for theoretical analysis and prediction. According to (1)–(5) and the probability trees in Fig. 3, the transition equations for different states can be developed by utilizing MMC [51] in (6), where $P_i^{US}(t+1)$, $P_i^{A_1S}(t+1)$, $P_i^{A_2S}(t+1)$, and $P_i^{A_1G}(t+1)$ denote the possibility that the node i will be in the state of US, A_1S, A_2S, and A_1G at the following time step. The system will obtain the stationary solution when $t \to \infty$, and satisfying the following relations.

$$\begin{aligned}
P_i^{US}(t+1) &= P_i^{US}(t) = P_i^{US}, \\
P_i^{A_1S}(t+1) &= P_i^{A_1S}(t) = P_i^{A_1S}, \\
P_i^{A_2S}(t+1) &= P_i^{A_2S}(t) = P_i^{A_2S}, \\
P_i^{A_1G}(t+1) &= P_i^{A_1G}(t) = P_i^{A_1G},
\end{aligned} \tag{7}$$

TABLE I
DEFINITIONS OF SOME KEY QUANTITIES OR PARAMETERS IN THE PROPOSED GREEN BEHAVIOR MODEL.

Notation	Description
N	Number of nodes in networks.
a_i	The activity level of the node i in the information layer.
b_i	The activity level of the node i in the physical contact layer.
m_v	The number of connections the active nodes generate in a time step in the information layer.
m_p	The number of connections the active nodes generate in a time step in the physical contact layer.
η_v	Rescaling factor in the information layer.
η_p	Rescaling factor in the physical contact layer.
x_i	Activity potential of the node i in the information layer.
y_i	Activity potential of the node i in the physical contact layer.
$F_v(x)$	The distribution of the node's activity potential in the information layer.
$F_p(y)$	The distribution of the node's activity potential in the physical contact layer.
γ_v	Activity exponent of the information layer.
γ_p	Activity exponent of the physical contact layer.
λ_1	Positive information transmission rate.
λ_2	Negative information transmission rate.
δ_1	Positive information recovery rate.
δ_2	Negative information recovery rate.
β	Green behavior transmission rate.
β^{A_1}	Green behavior transmission rate for A_1 node.
β^{A_2}	Green behavior transmission rate for A_2 node.
β^{U}	Green behavior transmission rate for U node.
μ	Recovery rate of green nodes.
γ_1	The parameter controls the impact of the positive information on the physical contact layer.
γ_2	The parameter controls the impact of the negative information on the physical contact layer.
$r_i^{A_1}(t)$	The probability that the node i is not informed of positive information at the time step t.
$r_i^{A_2}(t)$	The probability that the node i is not informed of negative information at the time step t.
$q_i^{A_1}(t)$	The probability of the node i in A_1 is not infected by its neighbors in the physical layer at the time step t.
$q_i^{A_2}(t)$	The probability of the node i in A_2 is not infected by its neighbors in the physical layer at the time step t.
$q_i^{U}(t)$	The probability of the node i in U is not infected by its neighbors in the physical layer at the time step t.

where $P_i^{US}, P_i^{A_1S}, P_i^{A_2S}$, and $P_i^{A_1G}$ stand for the proportions of nodes in US, A_1S, A_2S, and A_1G at the steady state.

Identifying the extent to which green behavior can be widely adopted is significant. Then, we analyze the green behavior threshold β_c. If $\beta^U > \beta_c$, the green behavior begins to break out, while $\beta^U < \beta_c$, a large proportion of the people do not embrace green behavior. Hence, the proportion of green nodes is near 0 when β^U is close to β_c at the steady state, and we can assume that $P_i^{A_1G} = \epsilon_i \ll 1$. According to (3)–(5), the higher-order terms can be disregarded, yielding the following approximation.

$$\begin{aligned} q_i^{A_1}(t) &\approx 1 - \beta^{A_1} m_p \left(b_i \rho^{A_1G} + \theta_b^{A_1G}\right), \\ q_i^{A_2}(t) &\approx 1 - \beta^{A_2} m_p \left(b_i \rho^{A_1G} + \theta_b^{A_1G}\right), \\ q_i^{U}(t) &\approx 1 - \beta^{U} m_p \left(b_i \rho^{A_1G} + \theta_b^{A_1G}\right), \end{aligned} \tag{8}$$

where $\rho^{A_1G} = \sum_j P_j^{A_1G}(t)/N$, and $\theta_b^{A_1G} = \sum_j b_j P_j^{A_1G}/N$. For simplicity, we can define that $\alpha_i^{A_1} = \beta^{A_1} m_p \left(b_i \rho^{A_1G} + \theta_b^{A_1G}\right)$, $\alpha_i^{A_2} = \beta^{A_2} m_p \left(b_i \rho^{A_1G} + \theta_b^{A_1G}\right)$, and $\alpha_i^{U} = \beta^{U} m_p \left(b_i \rho^{A_1G} + \theta_b^{A_1G}\right)$. As a result, the expression of (6)

$$\begin{aligned} P_i^{US}(t+1) &= P_i^{A_1S}(t)\,\delta_1 q_i^U(t) + P_i^{A_2S}(t)\,\delta_2 q_i^U(t) + P_i^{A_1G}(t)\,\delta_1\mu + P_i^{US}(t)\,r_i^{A_1}(t)\,r_i^{A_2}(t)\,q_i^U(t) \\ P_i^{A_1G}(t+1) &= P_i^{A_1S}(t)\left\{\delta_1\left[1-q_i^U(t)\right] + (1-\delta_1)\left[1-q_i^{A_1}(t)\right]\right\} + P_i^{A_1G}(t)(1-\mu) + P_i^{US}(t)\left\{r_i^{A_1}(t)\,r_i^{A_2}(t)\right. \\ &\quad \left[1-q_i^U(t)\right] + \left[1-r_i^{A_1}(t) - \left(1-r_i^{A_1}(t)\right)\left(1-r_i^{A_2}(t)\right)\right]\left[1-q_i^{A_1}(t)\right] + \left[1-r_i^{A_2}(t)\right]\left[1-q_i^{A_2}(t)\right]\Big\} \\ &\quad + P_i^{A_2S}(t)\left\{\delta_2\left[1-q_i^U(t)\right] + (1-\delta_2)\left[1-q_i^{A_2}(t)\right]\right\} \\ P_i^{A_1S}(t+1) &= P_i^{A_1S}(t)(1-\delta_1)\,q_i^{A_1}(t) + P_i^{US}(t)\left[1-r_i^{A_1}(t) - \left(1-r_i^{A_1}(t)\right)\left(1-r_i^{A_2}(t)\right)\right] q_i^{A_1}(t) \\ &\quad + P_i^{A_1G}(t)(1-\delta_1)\,\mu \\ P_i^{A_2S}(t+1) &= P_i^{A_2S}(t)(1-\delta_2)\,q_i^{A_2}(t) + P_i^{US}(t)\left[1-r_i^{A_2}(t)\right] q_i^{A_2}(t) \end{aligned} \tag{6}$$

can be converted into the subsequent form:

$$\begin{aligned}
P_i^{US} &= P_i^{A_1S}\delta_1\left(1-\alpha_i^U\right)+P_i^{A_2S}\delta_2\left(1-\alpha_i^U\right)\\
&\quad+P_i^{A_1G}\delta_1\mu+P_i^{US}r_i^{A_1}r_i^{A_2}\left(1-\alpha_i^U\right),\\
P_i^{A_1G} &= P_i^{A_1S}\left[\delta_1\alpha_i^U+\left(1-\delta_1\right)\alpha_i^{A_1}\right]+P_i^{A_2S}\left[\delta_2\alpha_i^U\right.\\
&\quad\left.+\left(1-\delta_2\right)\alpha_i^{A_2}\right]+P_i^{US}\left[\left(1-r_i^{A_1}\right)r_i^{A_2}\alpha_i^{A_1}\right.\\
&\quad\left.+r_i^{A_1}r_i^{A_2}\alpha_i^U+\left(1-r_i^{A_2}\right)\alpha_i^{A_2}\right]+P_i^{A_1G}\left(1-\mu\right),\\
P_i^{A_1S} &= P_i^{A_1S}\left(1-\delta_1\right)\left(1-\alpha_i^{A_1}\right)+P_i^{A_1G}\left(1-\delta_1\right)\mu\\
&\quad+P_i^{US}\left(r_i^{A_2}-r_i^{A_1}r_i^{A_2}\right)\left(1-\alpha_i^{A_1}\right),\\
P_i^{A_2S} &= P_i^{A_2S}\left(1-\delta_2\right)\left(1-\alpha_i^{A_2}\right)+P_i^{US}\left(1-r_i^{A_2}\right)\\
&\quad\left(1-\alpha_i^{A_2}\right).
\end{aligned}\tag{9}$$

Next, the higher-order components of (9) can be ignored to further simplify the equation.

$$\begin{aligned}
P_i^{US} &= P_i^{A_1S}\delta_1+P_i^{A_2S}\delta_2+P_i^{US}r_i^{A_1}r_i^{A_2},\\
P_i^{A_1S} &= P_i^{A_1S}\left(1-\delta_1\right)+P_i^{US}\left(r_i^{A_2}-r_i^{A_1}r_i^{A_2}\right),\\
P_i^{A_2S} &= P_i^{A_2S}\left(1-\delta_2\right)+P_i^{US}\left(1-r_i^{A_2}\right),\\
P_i^{A_1G} &= P_i^{A_1S}\left[\delta_1\alpha_i^U+\left(1-\delta_1\right)\alpha_i^{A_1}\right]+P_i^{A_2S}\left[\delta_2\alpha_i^U\right.\\
&\quad\left.+\left(1-\delta_2\right)\alpha_i^{A_2}\right]+P_i^{US}\left[\left(1-r_i^{A_1}\right)r_i^{A_2}\alpha_i^{A_1}\right.\\
&\quad\left.+r_i^{A_1}r_i^{A_2}\alpha_i^U+\left(1-r_i^{A_2}\right)\alpha_i^{A_2}\right]+P_i^{A_1G}\left(1-\mu\right).
\end{aligned}\tag{10}$$

Based on the first three equations in (10), the last equation in (10) can be simplified.

$$\begin{aligned}
\mu P_i^{A_1G} &= \alpha_i^U\left(P_i^{A_1S}\delta_1+P_i^{A_2S}\delta_2+P_i^{US}r_i^{A_1}r_i^{A_2}\right)\\
&\quad+\alpha_i^{A_1}\left[P_i^{A_1S}\left(1-\delta_1\right)+\left(1-r_i^{A_1}\right)r_i^{A_2}P_i^{US}\right]\\
&\quad+\alpha_i^{A_2}\left[P_i^{A_2S}\left(1-\delta_2\right)+P_i^{US}\left(1-r_i^{A_2}\right)\right]\\
&= \alpha_i^U P_i^{US}+\alpha_i^{A_1}P_i^{A_1S}+\alpha_i^{A_2}P_i^{A_2S}.
\end{aligned}\tag{11}$$

Next, (11) can be simplified as:

$$\begin{aligned}
\mu P_i^{A_1G} &= \beta^U m_p\left(b_i\rho^{A_1G}+\theta_b^{A_1G}\right)P_i^{US}+\beta^{A_1}m_p\\
&\quad\left(b_i\rho^{A_1G}+\theta_b^{A_1G}\right)P_i^{A_1S}+\beta^{A_2}m_p\left(b_i\rho^{A_1G}\right.\\
&\quad\left.+\theta_b^{A_1G}\right)P_i^{A_2S}\\
&= \beta m_p\left(b_i\rho^{A_1G}+\theta_b^{A_1G}\right)\left(P_i^{US}+P_i^{A_1S}\gamma_1\right.\\
&\quad\left.+P_i^{A_2S}\gamma_2\right).
\end{aligned}\tag{12}$$

Meanwhile, the system reaches a steady state when $P_i^{A_1S}+P_i^{A_1G}=P_i^{A_1}$, and $P_i^{A_2S}=P_i^{A_2}$. Given that the proportion of green nodes can be negligible when the value of β is close to β_c at the steady state, we can obtain $P_i^{A_1S}+P_i^{A_2S}\approx P_i^{A_1}+P_i^{A_2}$, and $P_i^{US}=1-P_i^{A_1S}-P_i^{A_2S}\approx 1-P_i^{A_2}-P_i^{A_1}$. Hence, in accordance with (12), we obtain the following equation:

$$\begin{aligned}
\mu P_i^{A_1G} &= \left(1-P_i^{A_2}-P_i^{A_1}+P_i^{A_1S}\gamma_1+P_i^{A_2S}\gamma_2\right)\\
&\quad\beta m_p\left(b_i\rho^{A_1G}+\theta_b^{A_1G}\right)\\
&= \left(1-P_i^{A_2}-P_i^{A_1}+P_i^{A_1}\gamma_1+P_i^{A_2}\gamma_2\right)\\
&\quad\beta m_p\left(b_i\rho^{A_1G}+\theta_b^{A_1G}\right)\\
&= \left[1-\left(1-\gamma_1\right)P_i^{A_1}-\left(\left(1-\gamma_2\right)P_i^{A_2}\right)\right]\\
&\quad\beta m_p\left(b_i\rho^{A_1G}+\theta_b^{A_1G}\right).
\end{aligned}\tag{13}$$

Next, (13) can be further expressed as:

$$\begin{aligned}
\mu P_i^{A_1G} &= \beta m_p\left[b_i\rho^{A_1G}-\left(1-\gamma_1\right)b_i\rho^{A_1G}P_i^{A_1}-\right.\\
&\quad\left(1-\gamma_2\right)b_i\rho^{A_1G}P_i^{A_2}+\theta_b^{A_1G}-\left(1-\gamma_1\right)P_i^{A_1}\\
&\quad\left.\theta_b^{A_1G}-\left(1-\gamma_2\right)P_i^{A_2}\theta_b^{A_1G}\right].
\end{aligned}\tag{14}$$

To obtain the proportion of the green node, we can take the average over all nodes, and obtain the next equation:

$$\mu\rho^{A_1G}=\frac{\mu}{N}\sum_i P_i^{A_1G}.\tag{15}$$

Combining (14) and (15), we get:

$$\begin{aligned}
\mu\rho^{A_1G} &= \beta m_p\left\{\rho^{A_1G}\left[\langle b\rangle-\left(1-\gamma_1\right)\theta_b^{A_1}-\left(1-\gamma_2\right)\theta_b^{A_2}\right]\right.\\
&\quad\left.+\theta_b^{A_1G}\left[1-\left(1-\gamma_1\right)\rho^{A_1}-\left(1-\gamma_2\right)\rho^{A_2}\right]\right\},
\end{aligned}\tag{16}$$

where $\theta_b^{A_2}=\sum_j b_j P_j^{A_2}/N$, and $\rho^{A_1}=\sum_i P_i^{A_1}/N$. To obtain a closed expression of $\theta_b^{A_1G}$, we multiply b_i on two sides of (14) and calculate the average across all nodes.

$$\begin{aligned}
\mu\theta_b^{A_1G} &= \beta m_p\left\{\rho^{A_1G}\left[\left\langle b^2\right\rangle-\left(1-\gamma_1\right)\theta_{b^2}^{A_1}-\left(1-\gamma_2\right)\theta_{b^2}^{A_2}\right]\right.\\
&\quad\left.+\theta_b^{A_1G}\left[\langle b\rangle-\left(1-\gamma_1\right)\theta_b^{A_1}-\left(1-\gamma_2\right)\theta_b^{A_2}\right]\right\},
\end{aligned}\tag{17}$$

where $\theta_{b^2}^{A_2}=\sum_j {b_j}^2 P_j^{A_2}/N$. The expressions of (16) and (17) can be as a matrix as follows:

$$H\begin{bmatrix}\rho^{A_1G}\\ \theta_b^{A_1G}\end{bmatrix}=\frac{\mu}{\beta m_p}\begin{bmatrix}\rho^{A_1G}\\ \theta_b^{A_1G}\end{bmatrix}.\tag{18}$$

The expression for H is shown in (19) at the bottom of this page.

As the green behavior begins to spread throughout the network at the steady state, the minimum value of β is β_c

$$H=\begin{bmatrix}\langle b\rangle-\left(1-\gamma_1\right)\theta_b^{A_1}-\left(1-\gamma_2\right)\theta_b^{A_2} & 1-\left(1-\gamma_1\right)\rho^{A_1}-\left(1-\gamma_2\right)\rho^{A_2}\\ \left\langle b^2\right\rangle-\left(1-\gamma_1\right)\theta_{b^2}^{A_1}-\left(1-\gamma_2\right)\theta_{b^2}^{A_2} & \langle b\rangle-\left(1-\gamma_1\right)\theta_b^{A_1}-\left(1-\gamma_2\right)\theta_b^{A_2}\end{bmatrix}.\tag{19}$$

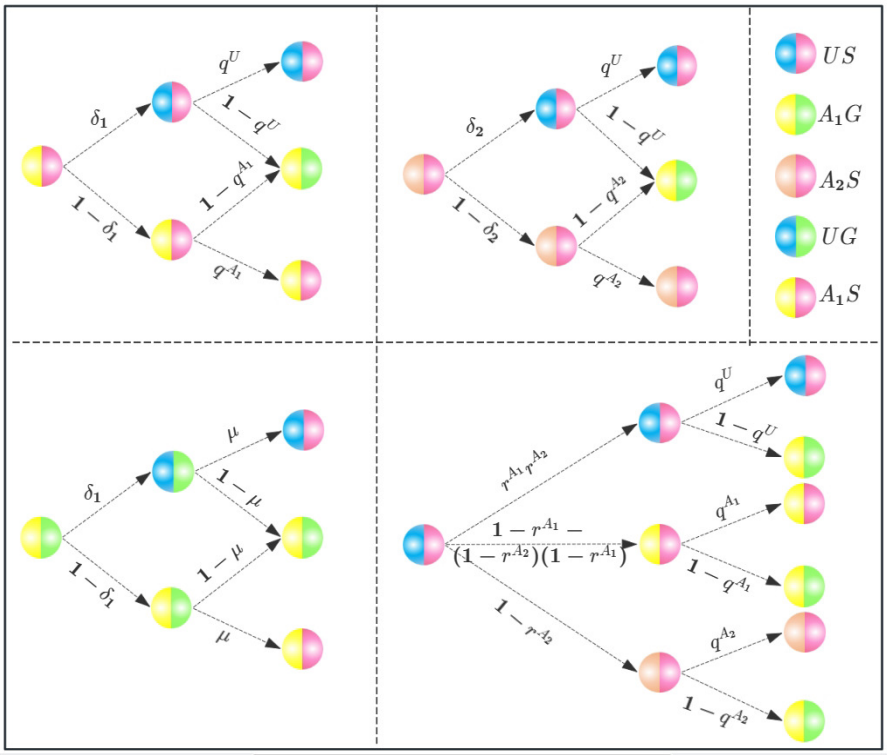

Fig. 3. The probability transition tree for the US, A_1S, A_2S, and A_1G nodes. UG is an intermediate state that will eventually disappear. Nodes in states A_1S and A_2S may forget or grow disinterested in the green information and return to the state US at the recovery rate δ_1 and δ_2, respectively. Moreover, r^{A_1} and r^{A_2} represent the probability that a node is not informed of positive and negative information, respectively. Similarly, q^{A_1} (q^{A_2} or q^U) stands for the probability that a node in A_1 (A_2 or U) is not infected by its neighbors in the physical layer. A green node will give up the green behavior with a recovery probability μ.

which satisfies (18) with $\begin{bmatrix} \rho^{A_1G} \\ \theta_b^{A_1G} \end{bmatrix} \neq 0$ [42]. Moreover, the value of f $\mu/(\beta_c m_p)$ is equivalent to the biggest eigenvalue of the matrix H. Then the biggest eigenvalue is:

$$\Lambda_{\max}(H) = \sqrt{x} + \langle b \rangle - (1-\gamma_1)\theta_b^{A_1} - (1-\gamma_2)\theta_b^{A_2},$$

where $x = \left[1-(1-\gamma_1)\rho^{A_1} - (1-\gamma_2)\rho^{A_2}\right]\left[\langle b^2\rangle - (1-\gamma_1)\theta_{b^2}^{A_1} - (1-\gamma_2)\theta_{b^2}^{A_2}\right]$.

As a result, we can get:

$$\begin{aligned}\beta_c &= \frac{\mu}{m_p \Lambda_{\max}(H)} \\ &= \frac{\mu}{m_p}\left[\sqrt{x} + \langle b \rangle - (1-\gamma_1)\theta_b^{A_1} - (1-\gamma_2)\theta_b^{A_2}\right]^{-1}.\end{aligned} \tag{20}$$

It is evident from (20) that the green behavior threshold is associated with the spread of two kinds of information. Additionally, the green behavior threshold of the proposed model is influenced by the parameter γ_1 and γ_2, the recovery probability μ, and the physical network's topological structure.

V. Numerical Simulations

Several simulations are performed in this section to validate the proposed model, coupling green behavior diffusion and information spreading. Firstly, we describe the variation of each node over time in synthetic networks and real-world networks. Secondly, the impact of various parameters in the upper and lower networks on green behavior spreading is investigated. Thirdly, the effect of relevant parameters on green behavior thresholds is analyzed. Fourthly, the influence of time-varying properties on the spread of green behavior is examined.

For the synthetic network, we construct the multiplex networks with 1,000 nodes by activity-driven model. Referring to [53] and [54], we set the activity exponent of different layers as $\gamma_p = \gamma_v = 2.1$, the number of connections that active nodes have produced as $m_v = m_p = 5$, and the rescaling factors as $\eta_v = \eta_p = 1$. It should be noted that unless certain parameters are chosen as variables, their values remain constant.

For the sake of verifying the practicality of the $UA_1A_2U - SGS$ model, we carry out some simulations on real-world time-varying multiplex networks. We supply the experiments of model propagation on Social Evolution Dataset, which is conducted by the MIT Media Lab [55]. The Social Evolution experiment tracked the everyday life of a whole undergraduate dormitory with mobile phones from October 2008 to May 2009. The data set is represented by a temporal duplex network, constituted by two different layers: A physical layer, formed by face-to-face interactions, and a digital layer built by sharing all tagged Facebook photos, or sharing blog/ live journal/ Twitter activities. Subsequently, we divide the period into independent intervals, extract subgraphs for each

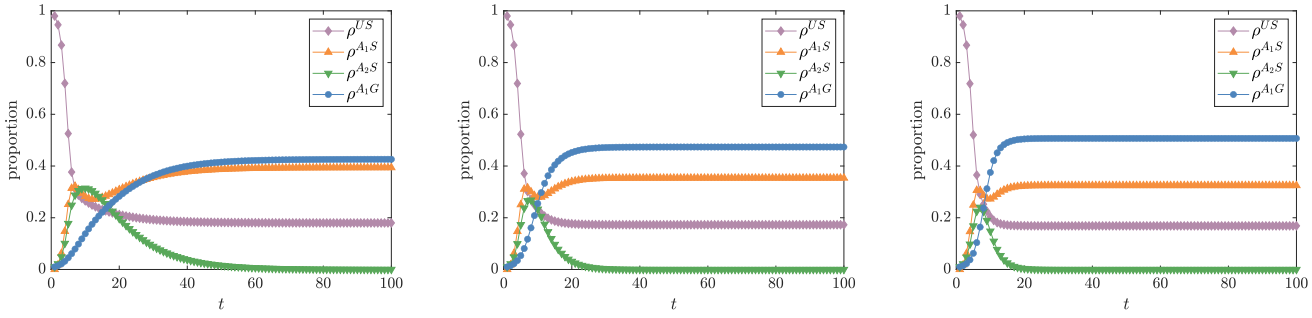

(a) (b) (c)

Fig. 4. The evolution of green behavior and information diffusion in synthetic time-varying multiplex networks. The fixed parameters are set as $\lambda_1 = \lambda_2 = 0.6$, $\delta_1 = \delta_2 = 0.3$, $\beta = 0.4$, and $\mu = 0.5$, which is the same as [56]. In panel (a), the settings are $\gamma_1 = 1.2, \gamma_2 = 0.2$. In panel (b), the settings are $\gamma_1 = 1.5, \gamma_2 = 0.5$. In panel (c), the settings are $\gamma_1 = 1.8, \gamma_2 = 0.8$. In all cases, the density of green individuals increases rapidly in the initial stages until it reaches a peak. This peak is influenced by the values of γ_1 and γ_2; higher values of γ_1 and γ_2 lead to a higher peak density of green individuals.

raw dataset, and generate four corresponding activity-driven networks. Similar to the method in [53], we measure the activity rate of each node as the number of interactions it performs in a given time interval, divided by the maximum number of interactions performed by all nodes during the same time interval.

A. The Trend of Change at Different Nodes

To more accurately depict the diffusion of green behavior and the correspondent information, we designate the evolution of green behavior and information diffusion over time in both synthetic networks and real-world networks. Specially, ρ^{A_1G} stands for the percentage of green individuals in the lower layer at the steady state. ρ^{US} stands for the percentage of susceptible individuals who are unaware of the green information at the steady state. ρ^{A_1S} and ρ^{A_2S} indicate the proportions of susceptible nodes that are aware of positive and negative green information at the steady state. In each experiment, the initial values of ρ^{A_1G}, ρ^{A_1S}, ρ^{A_2S}, and ρ^{US} are 0.1, 0, 0.1, and 0.98. According to the processes outlined in Fig. 1 and Fig. 3, we progress the interaction dynamics in the information and physical contact layers.

1) Synthetic networks: Fig. 4 illustrates the evolution of green behavior and information diffusion in synthetic time-varying multiplex networks, with three subplots (a, b, c) representing different parameter settings. In the above three cases, the green nodes increase rapidly, stabilizing at a significant proportion over time. The node that is susceptible and unaware of any information decreases correspondingly, indicating successful diffusion of green behavior. Individuals who are susceptible and aware of positive information initially increase and then stabilize, while A_2S nodes increase and then decrease to 0. Comparing Figs. 4(a), 4(b), and 4(c), the density of green individuals surges in the early stages until it peaks, with the peak value being higher for larger γ_1 and γ_2. This demonstrates that increasing γ_1 and γ_2 enhances the overall diffusion and stable adoption of green behavior in the network.

2) Real-world networks: Fig. 5 illustrates the evolution of green behavior and information diffusion in real-world networks. Comparing Fig. 4 with Fig. 5, the results of the real and synthetic data are consistent: the trend of the individual nodes is the same. In the above three cases, the green behavior nodes increase rapidly, reaching a stable proportion as time progresses. The US node decreases over time, indicating that fewer individuals remain susceptible as the green behavior spreads. A_2S nodes will eventually disappear from the system, and the trend for A_1S nodes as well as A_1G nodes is quite similar. Comparing the three subplots in Fig. 5, the greater the values of the parameter γ_1 and γ_2, the more people adopt green behaviors.

B. Validation and Sensitivity Analysis

Here, we conduct experiments to examine the effects of some key parameters of the $UA_1A_2U - SGS$ model. We designate the density of green nodes in the lower layer at the steady state as ρ^G. Moreover, ρ^{A_1} and ρ^{A_2} are employed to depict the percentage of nodes in the upper layer that are aware of positive and negative green information at the steady state. In the computations of the MMC iterative, we define $\rho^G = \left(\sum_i P_i^{A_1G}\right)/N, \rho^{A_1} = \left[\sum_i \left(P_i^{A_1G} + P_i^{A_1S}\right)\right]/N$, and $\rho^{A_2} = \left(\sum_i P_i^{A_2S}\right)/N$.

1) Influence of parameters in physical contact layer on propagation: In order to verify our MMC theoretical analysis, we supplement the Monte Carlo (MC) simulations and compare them with the theoretical solution. Moreover, for the result of MC simulations, $\rho^G = N_{A_1G}/N, \rho^{A_1} = (N_{A_1G} + N_{A_1S})/N$, and $\rho^{A_2} = N_{A_2S}/N$, where N_{A_1G}, N_{A_1S}, and N_{A_2S} are the number of nodes at the states of A_1G, A_1S, and A_2S in the steady state, respectively.

Fig. 6 clearly depicts the changes in three states $\left(\rho^G, \rho^{A_1}, \rho^{A_2}\right)$ as functions of the transmission rate β which is obtained by MMC and MC. It is observed that the positive information and the green behavior simultaneously outbreak around the threshold β_c. Specifically, when $\beta < \beta_c$, the value of ρ^G and ρ^{A_1} is 0, and when $\beta > \beta_c$, the values of ρ^G and ρ^{A_1} begin to increase. Additionally, the proportion of nodes that disseminate negative information starts to decrease when β approaches the threshold β_c. Possible explanations

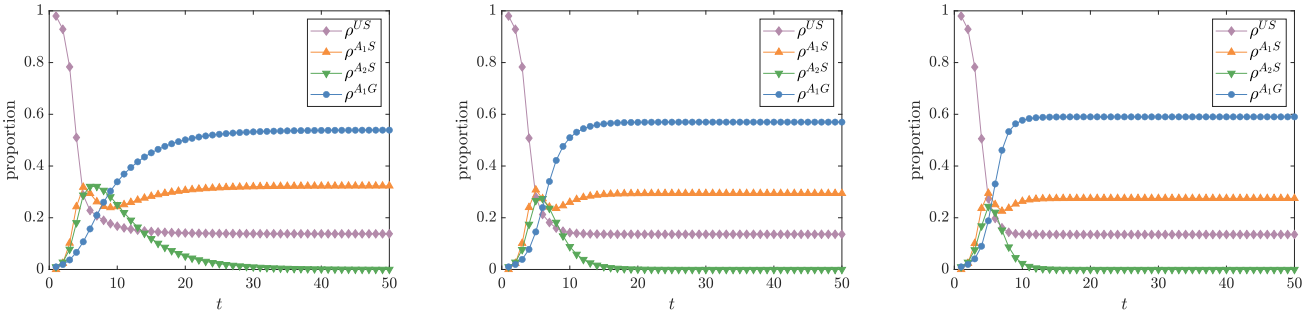

(a) (b) (c)

Fig. 5. The evolution of green behavior and information diffusion on the Social Evolution Dataset, which is conducted by the MIT Media Lab. The fixed parameters are set as $\lambda_1 = \lambda_2 = 0.6$, $\delta_1 = \delta_2 = 0.3$, $\beta = 0.4$, and $\mu = 0.5$. In panel (a), the settings are $\gamma_1 = 1.2, \gamma_2 = 0.2$. In panel (b), the settings are $\gamma_1 = 1.5, \gamma_2 = 0.5$. In panel (c), the settings are $\gamma_1 = 1.8, \gamma_2 = 0.8$. In all cases, the density of green individuals mounts up in the early stages until it reaches the maximum value, and the larger the γ_1 and γ_2, the larger this value is.

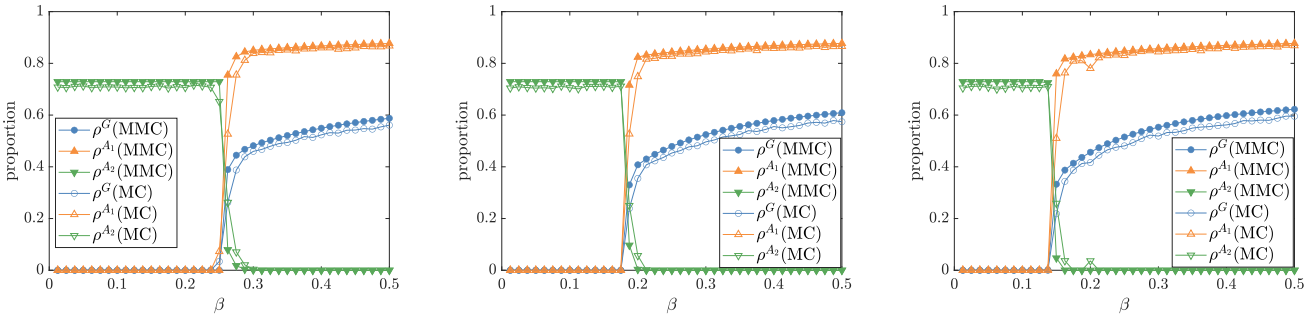

(a) (b) (c)

Fig. 6. The analysis of the outcomes achieved by MC and MMC with the increase of green behavior transmission rate β. The fixed parameters are set as $\lambda_1 = \lambda_2 = 0.6$, $\delta_1 = \delta_2 = 0.3$, and $\mu = 0.5$. In panel (a), the settings are $\gamma_1 = 1.2, \gamma_2 = 0.2$. In panel (b), the settings are $\gamma_1 = 1.5, \gamma_2 = 0.5$. In panel (c), the settings are $\gamma_1 = 1.8, \gamma_2 = 0.8$. In all cases, when $\beta > \beta_c$, the values of ρ^G and ρ^{A_1} begin to increase, and ρ^{A_2} starts to decrease as the value of β is increased, demonstrating the advantage of increasing the green behavior transmission rate in promoting green behavior spreading.

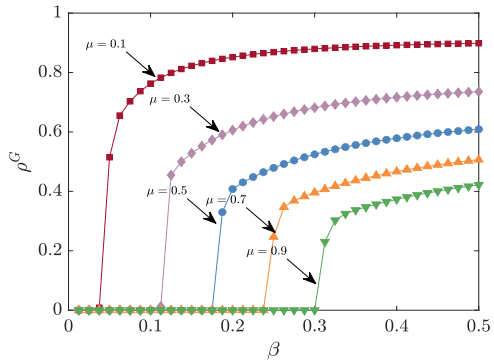

Fig. 7. Densities of the green nodes versus green behavior transmission rate under different recovery rates of green nodes. The fixed parameters are set as $\lambda_1 = \lambda_2 = 0.6$, $\delta_1 = \delta_2 = 0.3$, $\gamma_1 = 1.5$, and $\gamma_2 = 0.5$. As β increases, the density of green nodes increases, and lower recovery rates μ result in higher densities of green nodes.

for the above phenomenon can be concluded as follows. The proportion of green nodes grows as the transmission rate grows when $\beta > \beta_c$. Once the individuals transition into green nodes, they will promptly disseminate positive information. Thus, the positive information and the green behavior outbreak around the threshold β_c simultaneously. Conversely, when the green behavior transmission rate is high, people are more likely to adopt green behavior. This will lead to more people spreading positive messages, thus suppressing the spread of negative information. Hence, an excellent way to prompt the outbreak of green behavior is by suppressing the transmission of negative information. Additionally, comparing Figs. 6(a), 6(b), and 6(c), the threshold for the green behavior is smaller, and the green behavior prevalence increases. The reason is the greater the values of the parameter γ_1 and γ_2, the greater the green behavior transmission rate for A_1 and A_2 nodes. Thus, more effective dissemination of information will help to green behavior outbreaks and expand its prevalence.

Fig. 7 effectively illustrates the sensitivity of green behavior density to varying green behavior transmission rates and recovery rates of green nodes. This figure is essential for conducting a sensitivity analysis to understand how varying recovery rates impact the spread and stabilization of green behavior in the time-varying multiplex networks. It is clear to see that for all values of μ, as the propagation rate β increases, the density of green nodes ρ^G increases, indicating a higher adoption rate of green behavior. The sensitivity of ρ^G to changes in β varies with μ; lower values of μ show a

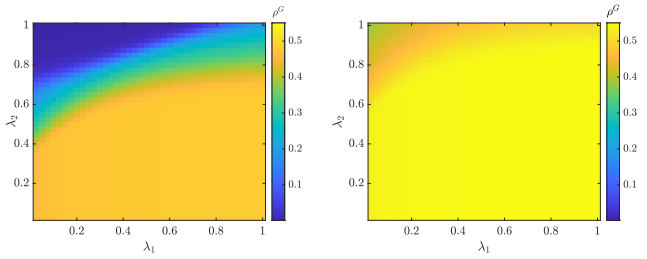

Fig. 8. The heat maps of green nodes as a function of positive and negative information spreading rate. The parameters are $\delta_1 = \delta_2 = 0.3$, $\mu = 0.5$,$\gamma_1 = 1.2$, $\gamma_2 = 0.2$. In panel (a), the fixed parameters are $\beta = 0.3$. In panel (b), the fixed parameters are $\beta = 0.4$. As λ_1 increases and λ_2 decreases, the density of green behavior increases, indicating inhibiting the transmission of negative information and promoting the propagation of positive information are effective in encouraging the adoption of green behavior.

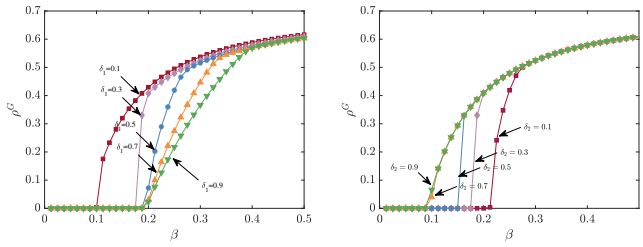

Fig. 9. Densities of the green nodes versus green behavior transmission rate under positive or negative information recovery rate. The fixed parameters are set as $\lambda_1 = \lambda_2 = 0.6$, $\gamma_1 = 1.5, \gamma_2 = 0.5$, and $\mu = 0.5$. In panel (a), the fixed parameters are $\delta_2 = 0.3$. In panel (b), the fixed parameters are $\delta_1 = 0.3$. Both panels show a rapid increase in ρ^G with increasing β; lower values of δ_1 and higher values of δ_2 result in a rapid increase in the density of green nodes.

steeper increase in ρ^G with β, while higher values of μ show a more gradual increase. The reason is that individuals who adopt green behavior are less likely to revert with a lower recovery rate μ, allowing the behavior to spread and stabilize quickly. Yet, higher recovery rates μ make it challenging for green behavior to spread and stabilize, as individuals are more likely to revert from green behavior. Hence, lower recovery rates enhance the spread and stabilization of green behavior, while higher recovery rates hinder it.

2) Influence of parameters in information layer on propagation: Subsequently, it is imperative to examine the impact of the rate at which positive or negative information is transmitted on green behavior prevalence. Fig. 8 clearly depicts the prevalence of green behavior within a wide range of λ_1 and λ_2. For a fixed λ_1, when the value of λ_2 is greater than a particular value, the prevalence of green behavior decreases as λ_2 increases. Moreover, as λ_1 gets smaller, the specific value gets smaller and A_2 can inhibit the spread of green behaviors at a smaller spread rate. The following are explanations that may account for this phenomenon: the role of negative information keeps increasing and the role of positive information keeps being weakened as the increase of negative information transmission, leading to the green behavior prevalence decreases; moreover, when the value of λ_1 is large, the spread of negative information would have to be very high to inhibit the spread of green behavior. Furthermore, comparing panel (a) with panel (b) in Fig. 8, the value of λ_2 must be at least 0.6 to exert a dominant effect of inhibition in panel (b), since a large number of nodes adopt green behavior leads to more positive information in networks, and negative information is hard to propagate based on the high green behavior transmission rate. Generally, it is possible to improve green behavior prevalence by inhibiting the transmission of negative information and promoting the propagation of positive information.

Fig. 9 effectively illustrates the sensitivity of green behavior density to varying green behavior transmission rates and positive or negative information recovery rates. This figure is divided into two panels: Panel (a) focuses on five positive information recovery rates, while panel (b) focuses on five negative recovery rates. In panel (a), lower positive recovery rates δ_1 result in a rapid increase in the density of green nodes ρ^G at lower values of β. Yet, higher positive recovery rates δ_1 make it more challenging for green behavior to spread, requiring higher β values to reach similar densities. In panel (b), higher negative recovery rates δ_2 also result in a rapid increase in ρ^G. Contrary to the trend observed with δ_1, lower negative recovery rates δ_2 hinder the spread of green behavior, requiring higher β values to achieve comparable densities. For both panels, when β is large, the final density of green nodes ρ^G shows little variation across different values of δ_1 and δ_2, indicating that the transmission rate β plays a dominant role in determining the equilibrium density of green behavior. Therefore, lower positive information recovery rates enhance the spread and stabilization of green behavior, while lower negative information recovery rates hinder it. However, when the green behavior transmission rate β is sufficiently high, the final density of green nodes becomes less sensitive to variations in information recovery rates, emphasizing the critical role of transmission rate in behavior adoption.

C. Influence of Related Parameters on Green Behavior Threshold

In this subsection, we explore different parameters on the green behavior threshold computed by (20). In Fig. 10(a), when the values of δ_1, δ_2, μ and λ_2 are fixed, the threshold β_c exhibits a progressively decreasing trend as the value of λ_1 is varied from 0.3 to 0.9. Similarly, when δ_1, δ_2, μ, and λ_1 are fixed, the threshold β_c increases as λ_2 increases from 0.1 to 0.6. Therefore, it is possible to prompt the outbreak of green behavior by preventing the diffusion of negative information and facilitating the spread of positive information. In Fig. 10(b), while keeping the parameters λ_1, λ_2, δ_1 and μ constant, the green behavior threshold β_c decreases as δ_2 increases, whereas it decreases as δ_1 decreases when λ_1, λ_2, δ_2 and μ are fixed. Hence, reducing the rates of forgetting positive information and increasing the rates of forgetting negative information can be considered beneficial approaches to encourage the outbreak of green behavior. Furthermore, the threshold of green behavior also increases as the recovery

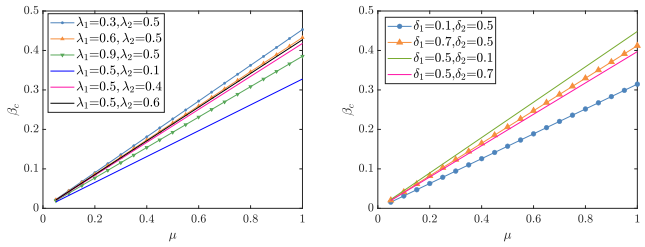

(a) (b)

Fig. 10. Green behavior threshold as a function of recovery rate of green nodes μ. Panel (a) depicts the relationship between the green behavior threshold and recovery rate of green nodes under the different values of the information transmission rate. The parameters are set as $\delta_1 = \delta_2 = 0.05$. Panel (b) depicts the relationship between the green behavior threshold and recovery rate of green nodes under the different values of the information recovery rate. The parameters that control the impact of the information on the physical contact layer are set as $\gamma_1 = 1.2$ and $\gamma_2 = 0.8$ in panel (a) and panel (b). In both panels, thresholds increase as the recovery rates of green nodes increase.

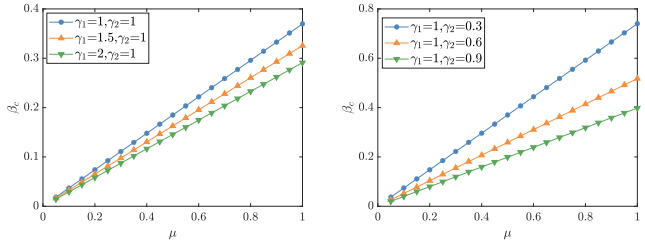

(a) (b)

Fig. 11. Green behavior threshold as a function of recovery rate of green nodes μ for different values of γ_1 and γ_2. The fixed parameters are set as $\lambda_1 = \lambda_2 = 0.5, \delta_1 = \delta_2 = 0.01$. In panel (a), γ_2 remains constant and γ_1 changes. In panel (b), γ_1 remains constant and γ_2 changes. The threshold increases as the recovery rate increases. Moreover, the larger values of γ_1 and γ_2 result in a lower threshold.

rate μ increases. Therefore, it is also possible to prompt the outbreak of green behavior by reducing the probability of abandoning green behavior.

Additionally, we analyze the impact of the γ_1 and γ_2 on the green behavior threshold in Fig. 11. It is clear to see that the green behavior threshold gradually decreases as γ_1 increases while other parameters are fixed in Fig. 11(a). This implies that the stronger the influence of positive information, the more people are willing to adopt green behavior and the lower the threshold is. Conversely, in Fig. 11(b), the stronger the inhibitory effect of negative information, the lower the probability of an individual adopting green behavior, and the green behavior threshold increases. As a result, mitigating the influence of negative messages and increasing the impact of positive information can facilitate the outbreak of green behavior.

D. Influence of Time-varying Properties on Green Behavior Diffusion

Subsequently, we try to figure out how the changing structure of the adaptive network, including the contact capacity and activity heterogeneity, affects the process of coupled dynamics. Since there are two types of information and their roles are opposite in the system, the relationship between green behavior spreading and topological structure is different when different information plays a dominant role. Hence, the simulation will be discussed in the following two aspects.

- Positive information is predominant: Positive information plays a bigger role than negative information.
- Negative information is predominant: Negative information plays a bigger role than positive information.

1) Influence of nodal activity heterogeneity on green behavior diffusion: Fig. 12 depicts how the green behavior threshold and the final green behavior proportion are affected by the value of γ_v. In Fig. 12(a), there are two types of relationships between the threshold and activity exponent of the information layer. When λ_1 is larger than λ_2, it is visual to see the green behavior threshold increases with the activity exponent of the physical contact layer γ_v. Conversely, when λ_2 is larger than λ_1, the green behavior threshold decreases with γ_v. The principal reason for this phenomenon is that a higher activity exponent results in less heterogeneity of the nodes, and an increase in γ_v leads to a weakening effect of the node A_1 when λ_1 is larger than λ_2. Hence, weakened dissemination of positive messages leads to a higher green behavior threshold. Conversely, when the negative information plays a dominant role in the upper layer, an increase in γ_v results in a decrease in the weakening effect of negative information in the system. Moreover, to analyze the effect of the final green behavior proportion, we selected one set of parameters from the three sets of parameters for each type. Specifically, we choose $\lambda_1 = 0.8, \lambda_2 = 0.2$ when positive information plays a bigger role than negative information; and we choose $\lambda_1 = 0.2, \lambda_2 = 0.8$ when negative information plays a bigger role than positive information. In Fig. 12(b), when β is certain and greater than the propagation threshold, the final green behavior density decreases slightly as γ_v increases, while the trend is reversed in Fig. 12(c). As a result, when positive information is predominant, we should decrease the activity exponent of the information layer; when negative information is predominant in the system, we should increase the activity exponent of the information layer.

Fig. 13 depicts how the green behavior threshold and the final green behavior proportion are affected by the value of γ_p. In Fig. 13(a), it is clear that the green behavior threshold increases monotonically with the activity exponent of the information layer γ_p. When γ_p is fixed, the larger λ_1 is, the smaller the threshold is. A possible explanation for the above phenomenon is that a lower activity exponent results in more heterogeneity of the nodes. Nodes are highly active when the nodal activities are more heterogeneous. These nodes are capable of sustaining their activities in sequential time steps, which provides the spreading process with constant impetus. Then, the smaller the γ_p, the more conducive the spread of green behavior. Besides, the higher the propagation rate of positive information, the more nodes will become A_1 and propagate green behavior at a higher rate, thus contributing to the outbreak of green behavior. In Figs. 13(b) and 13(c), regardless of who has a strong role in the upper layer, when β is certain and greater than the propagation threshold, the larger

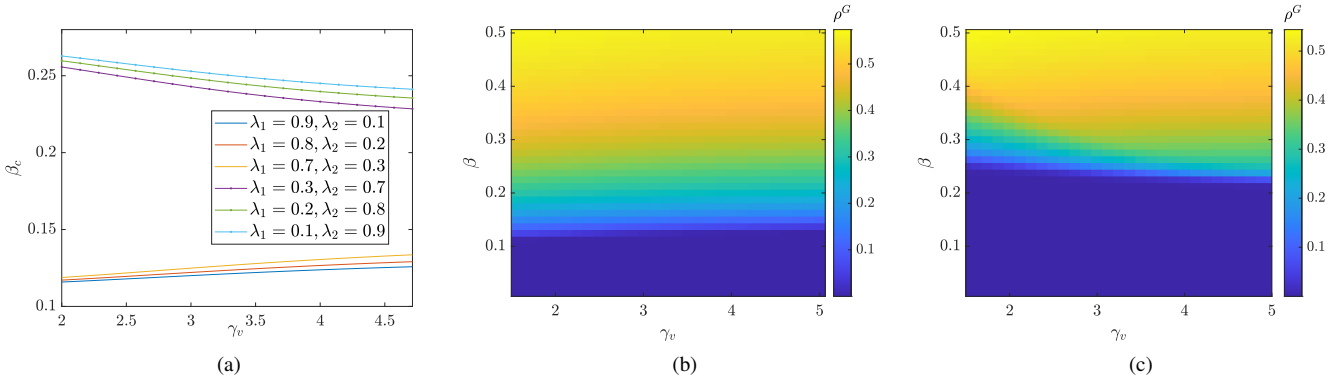

(a) (b) (c)

Fig. 12. The impact of activity heterogeneity on green behavior propagation in the information layer. The parameters are set as $\delta_1 = \delta_2 = \mu = 0.5$, $\gamma_1 = 2, \gamma_2 = 0.5$, $\gamma_p = 2.1$. (a) The relationship between green behavior threshold β_c and the activity exponent γ_v for different values of λ_1 and λ_2. (b) The relationship between the density of green behavior nodes ρ^G versus the activity exponent γ_v and β when $\lambda_1 = 0.8$ and $\lambda_2 = 0.2$. (c) The relationship between the density of green behavior nodes ρ^G versus the activity exponent γ_v and β when $\lambda_1 = 0.2$, $\lambda_2 = 0.8$. When λ_1 is larger than λ_2, as the nodal activities in the information layer become more heterogeneous (corresponding to smaller values of γ_v), the green behavior threshold decreases and the final infection density increases slightly. When λ_2 is greater than λ_1, the result is reversed.

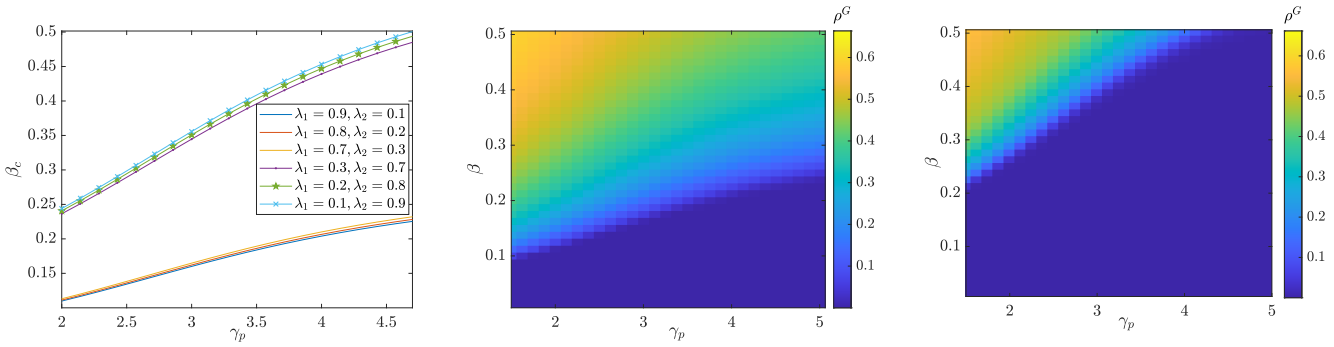

(a) (b) (c)

Fig. 13. The impact of activity heterogeneity on green behavior propagation in the physical contact layer. The parameters are set as $\delta_1 = \delta_2 = \mu = 0.5$, $\gamma_1 = 2, \gamma_2 = 0.5$, $\gamma_v = 2.1$. (a) The relationship between the green behavior threshold β_c and the activity exponent γ_p for different values of λ_1 and λ_2. (b) The relationship between the density of green behavior nodes ρ^G versus the activity exponent γ_p and β when $\lambda_1 = 0.8, \lambda_2 = 0.2$. (c) The relationship between the density of green behavior nodes ρ^G versus the activity exponent γ_p and β when $\lambda_1 = 0.2, \lambda_2 = 0.8$. The threshold is raised and the final infection density is reduced as the value of γ_p is increased, demonstrating the disadvantage of reducing nodal activity heterogeneity in promoting the adoption of green behavior.

γ_p is, the smaller the final green behavior density is. That is to say, a smaller activity exponent leads to a greater density of green behavior. Therefore, increasing the heterogeneity of the nodal activities in the physical contact layer can prompt green behavior spreading.

2) Influence of contact capacity on green behavior diffusion: Fig. 14 depicts how the green behavior threshold and the final green behavior density are affected by the value of m_v. In Fig. 14(a), when λ_1 is larger than λ_2, the value of green behavior threshold decreases and then increases or stabilizes as m_v increases. Additionally, when λ_2 is larger than λ_1, the value of green behavior threshold increases as m_v increases until saturation. The primary cause of this phenomenon is that when λ_1 is larger than λ_2, A_1 will connect more nodes as m_v increases, leading to more nodes supporting green behavior. At this point, the propagation threshold decreases. However, when m_v increases to a certain level, A_2 also connects more nodes, and the inhibitory effect of A_2 starts to manifest itself, leading to a rise or stabilization of the threshold value. In addition, when λ_2 is larger than λ_1, negative information plays a dominant role in the upper layer, and the inhibitory effect of negative information increases as m_v increases. In Fig. 14(b), when $\lambda_1 > \lambda_2$, the density of green behavior increases as m_v increases until saturation. In Fig. 14(c), when $\lambda_1 < \lambda_2$, the density of green behavior increases and then decreases as m_v increases. As a result, when negative information plays a dominant role, we should decrease the contact capacity of the information layer; when positive information plays a dominant role in the system, we should increase the contact capacity of the information layer.

Fig. 15 depicts how the green behavior threshold and the final green behavior proportion are affected by the value of m_p. The threshold for green behavior decreases with the number of links generated by the active nodes increases in the physical contact layer in a time step, regardless of the size relationship between λ_1 and λ_2. A possible explanation for the above phenomenon is that when m_p is larger, the active nodes will generate more edges and connect more nodes in the physical contact layer, facilitating the propagation of green behavior. Thus, the propagation threshold is smaller and the

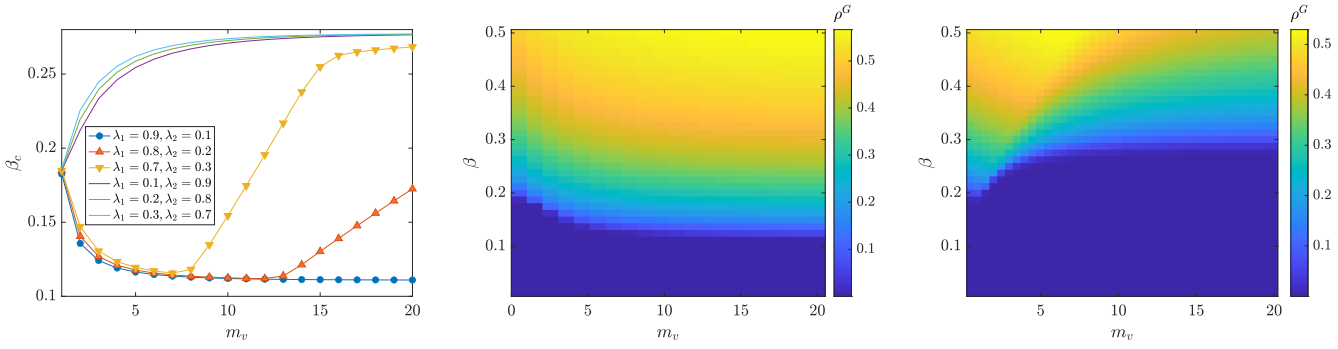

(a) (b) (c)

Fig. 14. The influence of contact capacity on green behavior propagation in the information layer. The parameters are set as $\delta_1 = \delta_2 = \mu = 0.5, \gamma_1 = 2$, $\gamma_2 = 0.5$. (a) The relationship between green behavior threshold β_c and the contact capacity m_v for different values of λ_1 and λ_2. (b) The relationship between the density of green behavior nodes ρ^G versus the contact capacity m_v and β when $\lambda_1 = 0.8, \lambda_2 = 0.2$. (c) The relationship between the density of green behavior nodes ρ^G versus the contact capacity m_v and β when $\lambda_1 = 0.2, \lambda_2 = 0.8$. When λ_1 is larger than λ_2, the green behavior threshold is smaller than λ_1 is less than λ_2, and the prevalence of green behavior under the two scenarios is the opposite.

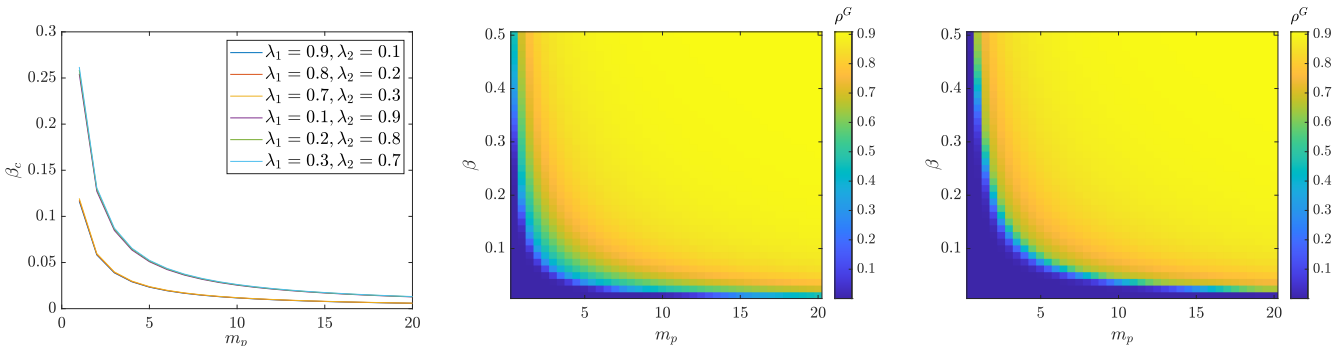

(a) (b) (c)

Fig. 15. The impact of contact capacity on green behavior propagation in the physical contact layer. The parameters are set as $\delta_1 = \delta_2 = 0.5, \mu = 0.1, \gamma_1 = 2, \gamma_2 = 0.5$. (a) The relationship between green behavior threshold β_c and the contact capacity m_p for different values of λ_1 and λ_2. (b) The relationship between the density of green behavior nodes ρ^G versus the activity exponent m_p and β when $\lambda_1 = 0.8, \lambda_2 = 0.2$. (c) The relationship between the density of green behavior nodes ρ^G versus the contact capacity m_p and β when $\lambda_1 = 0.2, \lambda_2 = 0.8$. As the contact capacity in the physical contact layer increases, the green behavior threshold decreases, and the final infection density tends to increase.

density of green behaviors is greater. Therefore, enhancing the contact capacity of the nodes in the physical contact layer can prompt green behavior diffusion.

VI. Conclusion

In this paper, the $UA_1A_2U - SGS$ model in time-varying multiplex networks is proposed to investigate the features of green behavior diffusion under the impact of positive and negative information. In time-varying multiplex networks, one layer describes the positive and negative information diffusion and the other represents the green behavior spreading. Based on MMC, we build the probability transition equations and calculate the green behavior threshold of the model. Then, experiments are carried out to confirm the preciseness and theoretical predictions of the new model. It reveals that the prevalence of green behavior can be promoted by restraining the negative information transmission rate and recovery rate of the green nodes while facilitating the positive information transmission rate and green behavior transmission rate. Additionally, reducing the positive information recovery rate and the recovery rate of the green nodes, and increasing the rates of forgetting negative information are beneficial for encouraging the outbreak of green behavior. Moreover, we investigate the structure of the time-varying model that affects green behavior propagation. In the physical contact layer, higher contact capacity and greater activity heterogeneity significantly facilitate green behavior spreading. In the information layer, when negative information plays a dominant role, the smaller contact capacity and the weaker activity heterogeneity can promote green behavior diffusion; when positive information plays a dominant role, the larger contact capacity and the stronger activity heterogeneity of individuals can promote green behavior diffusion.

This paper provides a general framework to investigate green behavior diffusion in time-varying multiplex networks, providing some insightful analysis of actual situations and helping develop effective strategies to prompt green behavior spreading. The two-layer approach, which separately analyzes information diffusion and behavior spreading, allows for a detailed examination of the interplay between positive and negative information and green behavior adoption.

There are several limitations of this paper, which also casts light on future research directions. Firstly, the analysis is at a generalized level and does not consider the heterogeneity between different green behaviors or individual differences. Further work should focus on a special green behavior, with the consideration of individual heterogeneity. Secondly, the impact of external factors, such as social influence and media effects, is not explicitly considered in our model. Further work should explore the role of external factors to gain a more comprehensive understanding of green behavior adoption and refine intervention strategies.

REFERENCES

[1] X. Jiang and D. Guan, "Determinants of global CO2 emissions growth," *Appl. Energy.*, vol. 184, pp. 1132–1141, Dec. 2016.

[2] H. Yin, Z. Wang, and Z. Xu, "Transmission mechanism and influencing factors of green behavior in dynamic multiplex networks," *IEEE Access*, vol. 9, pp. 104382–104394, 2021.

[3] O. Artime *et al.*, "Robustness and resilience of complex networks," *Nat. Rev. Phys.*, vol. 6, no. 2, pp. 114–131, Jan. 2024.

[4] Y. Li, H. Gao, Y. Gao, J. Guo, and W. Wu, "A Survey on influence maximization: From an ML-based combinatorial optimization," *ACM Trans. Knowl. Discov. Data*, vol. 17, no. 9, pp. 1–50, Nov. 2023.

[5] X.-L. Sun, Y.-G. Wang, and L.-Q. Cang, "Correlation and trust mechanism-based rumor propagation model in complex social networks," Chin. Phys. B, vol. 31, no. 5, p. 050202, 2022.

[6] X. Gao, and L. Tian, "Effects of awareness and policy on green behavior spreading in multiplex networks," *Physica A*, vol. 514, pp. 226–234, Jan. 2019.

[7] C. Xia *et al.*, "A new coupled disease-awareness spreading model with mass media on multiplex networks," *Info. Sci.*, vol. 471, pp. 185–200, Jan. 2019.

[8] J. Gao, S. V. Buldyrev, H. E. Stanley, and S. Havlin, "Networks formed from interdependent networks," *Nat. Phys.*, vol. 8, no. 1, pp. 40–48, Jan. 2012.

[9] J. Guo, Q. Ni, W. Wu, and D.-Z. Du, "Composite community-aware diversified influence maximization with efficient approximation," *IEEE ACM Trans Netw.*, vol. 32, no. 2, pp. 1584–1599, Apr. 2024.

[10] T. Chen, S. Yan, J. Guo, and W. Wu, "ToupleGDD: A fine-designed solution of influence maximization by deep reinforcement learning," *IEEE Trans. Comput. Soc. Syst.*, vol. 11, no. 2, pp. 2210–2221, Apr. 2024.

[11] W. Li, L. Tian, X. Gao, and B. Pan, "Impacts of information diffusion on green behavior spreading in multiplex networks," *J. Clean. Prod.*, vol. 222, pp. 488–498, Jun. 2019.

[12] X. Li, J. Du, and H. Long, "Dynamic analysis of international green behavior from the perspective of the mapping knowledge domain," *Environ. Sci. Pollut. Res.*, vol. 26, no. 6, pp. 6087–6098, Feb. 2019.

[13] I. Mishkovski, M. Mirchev, S. Scepanovic, and L. Kocarev, "Interplay between spreading and random walk processes in multiplex networks," *IEEE Trans. Circuits Syst. I*, vol. 64, no. 10, pp. 2761–2771, Oct. 2017.

[14] Z. Ding *et al.*, "Factors affecting low-carbon consumption behavior of urban residents: A comprehensive review," *Resour. Conserv. Recycl.*, vol. 132, pp. 3–15, May 2018.

[15] J. Geng, R. Long, H. Chen, and W. Li, "Exploring the motivation-behavior gap in urban residents' green travel behavior: A theoretical and empirical study," *Resour. Conserv. Recycl.*, vol. 125, pp. 282–292, Oct. 2017.

[16] R. Tolley, "Green campuses: Cutting the environmental cost of commuting," *J. Transp. Geogr.*, vol. 4, no. 3, pp. 213–217, Sep. 1996.

[17] W. Wymer and M. J. Polonsky, "The limitations and potentialities of green marketing," *J. Nonprofit Public Sect. Mark.*, vol. 27, no. 3, pp. 239–262, Jul. 2015.

[18] H. Yang, C. Gu, M. Tang, S.-M. Cai, and Y.-C. Lai, "Suppression of epidemic spreading in time-varying multiplex networks," *Appl. Math. Model.*, vol. 75, pp. 806–818, Nov. 2019.

[19] M. Karsai, N. Perra, and A. Vespignani, "Time varying networks and the weakness of strong ties," *Sci. Rep.*, vol. 4, no. 1, p. 4001, Feb. 2014.

[20] P. Holme and J. Saramäki, "Temporal networks," *Phys. Rep.*, vol. 519, no. 3, pp. 97–125, Oct. 2012.

[21] H. Guo, Q. Yin, C. Xia, and M. Dehmer, "Impact of information diffusion on epidemic spreading in partially mapping two-layered time-varying networks," *Nonlinear Dyn.*, vol. 105, no. 4, pp. 3819–3833, Sep. 2021.

[22] L. Zhang, Y. Wang, and Q. Wang, "Synchronization for time-varying complex dynamical networks with different-dimensional nodes and non-dissipative coupling," *Commun Nonlinear Sci Numer Simul*, vol. 24, no. 1, pp. 64–74, Jul. 2015.

[23] L. Varela-Candamio, I. Novo-Corti, and M. T. García-Álvarez, "The importance of environmental education in the determinants of green behavior: A meta-analysis approach," *J. Clean. Prod.*, vol. 170, pp. 1565–1578, Jan. 2018.

[24] F. Belaid and T. Garcia, "Understanding the spectrum of residential energy-saving behaviours: French evidence using disaggregated data," *Energy Econ.*, vol. 57 pp. 204-214, Jun. 2016.

[25] S. Jin, X. Ma, and W. Yue, "Energy-saving strategy for green cognitive radio networks with an LTE-advanced structure," *J. Commun. Netw.*, vol. 18, no. 4, pp. 610–618, Aug. 2016.

[26] S. Matsumoto and H. Kawashima, "Fundamental study on effect of preceding vehicle information on fuel consumption reduction of a vehicle group," *J. Commun. Netw.*, vol. 15, no. 2, pp. 173–178, Apr. 2013.

[27] D. Li, J. Du, M. Sun, and D. Han, "How conformity psychology and benefits affect individuals' green behaviours from the perspective of a complex network," *J. Clean. Prod.*, vol. 248, p. 119215, Mar. 2020.

[28] Y. Wang, J. R. Huscroft, B. T. Hazen, and M. Zhang, "Green information, green certification and consumer perceptions of remanufctured automobile parts," *Resour. Conserv. Recycl.*, vol. 128, pp. 187–196, Jan. 2018.

[29] S. Kyoi and K. Mori, "Development of policy measures for diffusing human pro-environmental behavior in social networks—Computer simulation of a dynamic model of mutual learning," *World Dev. Sustain.*, vol. 4, p. 100118, Jun. 2024.

[30] T. Althoff, P. Jindal, and J. Leskovec, "Online actions with offline impact: How online social networks influence online and offline user behavior," in *Proc. ACM WSDM*, 2017.

[31] W. Li, L. Tian, and H. Batool, "Impact of negative information diffusion on green behavior adoption," *Resour. Conserv. Recycl.*, vol. 136, pp. 337–344, Sep. 2018.

[32] R. M. Bond *et al.*, "A 61-million-person experiment in social influence and political mobilization," *Nature*, vol. 489, no. 7415, pp. 295–298, Sep. 2012.

[33] D. Centola, "The spread of behavior in an online social network experiment," *Science*, vol. 329, no. 5996, pp. 1194–1197, Sep. 2010.

[34] L. Yang, Z. Li, and A. Giua, "Containment of rumor spread in complex social networks," *Info. Sci.*, vol. 506, pp. 113–130, Jan. 2020.

[35] X. Gao, L. Tian, and W. Li, "Coupling interaction impairs knowledge and green behavior diffusion in complex networks," *J. Clean. Prod.*, vol. 249, p. 119419, Mar. 2020.

[36] P. Ji *et al.*, "Signal propagation in complex networks," *Phys. Rep.*, vol. 1017, pp. 1–96, May 2023.

[37] S. Liu, N. Perra, M. Karsai, and A. Vespignani, "Controlling contagion processes in activity driven networks," *Phys. Rev. Lett.*, vol. 112, no. 11, p. 118702, Mar. 2014.

[38] A.-L. Barabási, "The origin of bursts and heavy tails in human dynamics," *Nature*, vol. 435, no. 7039, pp. 207–211, May 2005.

[39] E. Ubaldi, A. Vezzani, M. Karsai, N. Perra, and R. Burioni, "Burstiness and tie activation strategies in time-varying social networks," *Sci. Rep.*, vol. 7, no. 1, p. 46225, Apr. 2017.

[40] Y. Chai and Y. Wang, "Optimal control of information diffusion in temporal networks," *IEEE Trans. Netw. Serv. Manage.*, vol. 20, no. 1, pp. 104–119, Mar. 2023.

[41] I. Pozzana, K. Sun, and N. Perra, "Epidemic spreading on activity-driven networks with attractiveness," *Phys. Rev. E*, vol. 96, no. 4, p. 042310, Oct. 2017.

[42] Q. Guo *et al.*, "Epidemic spreading with activity-driven awareness diffusion on multiplex network," *Chaos*, vol. 26, no. 4, p. 043110, Apr. 2016.

[43] C. Li, Y. Zhang, and X. Li, "Epidemic threshold in temporal multiplex networks with individual layer preference," IEEE Trans. Netw. Sci. Eng., vol. 8, no. 1, pp. 814–824, Jan. 2021.

[44] P. Huang, X.-L. Chen, M. Tang, and S.-M. Cai, "Coupled dynamic model of resource diffusion and epidemic spreading in time-varying multiplex networks," *Complexity*, vol. 2021, pp. 1–11, Mar. 2021.

[45] H. Zhang, X. Chen, Y. Peng, G. Kou, and R. Wang, "The interaction of multiple information on multiplex social networks," *Info. Sci.*, vol. 605, pp. 366–380, Aug. 2022.

[46] Y.-H. Qin, Z.-D. Zhao, S.-M. Cai, L. Gao, and H. E. Stanley, "Dual-induced multifractality in online viewing activity," *Chaos*, vol. 28, no. 1, p. 013114, Jan. 2018.

[47] Q.-H. Liu, X. Xiong, Q. Zhang, and N. Perra, "Epidemic spreading on time-varying multiplex networks," *Phys. Rev. E*, vol. 98, no. 6, p. 062303, Dec. 2018.
[48] A. K. Moser, "Thinking green, buying green? Drivers of pro-environmental purchasing behavior," *J. Consum. Mark.*, vol. 32, no. 3, pp. 167–175, May 2015.
[49] I. None and S. Kumar Datta, "Pro-environmental concern influencing green buying: A study on indian consumers," *Int. J. Bus. Manage.*, vol. 6, no. 6, p. p124, Jun. 2011.
[50] Z. Wang, Q. Guo, S. Sun, and C. Xia, "The impact of awareness diffusion on SIR-like epidemics in multiplex networks," *Appl. Math. Comput.*, vol. 349, pp. 134–147, May 2019.
[51] C. Granell, S. Gómez, and A. Arenas, "Dynamical Interplay between awareness and epidemic spreading in multiplex networks," *Phys. Rev. Lett.*, vol. 111, no. 12, p. 128701, Sep. 2013.
[52] C. Granell, S. Gómez, and A. Arenas, "Competing spreading processes on multiplex networks: Awareness and epidemics," *Phys. Rev. E*, vol. 90, no. 1, p. 012808, Jul. 2014.
[53] N. Perra, B. Gonçalves, R. Pastor-Satorras, and A. Vespignani, "Activity driven modeling of time varying networks," *Sci. Rep.*, vol. 2, no. 1, p. 469, Jun. 2012.
[54] Y. Chai, Y.-G. Wang, J. Yan, and X.-L. Sun, "Intervention against information diffusion in static and temporal coupling networks," *Chin. Phys. B*, Feb. 2023.
[55] W. Dong, B. Lepri, and A. S. Pentland, "Modeling the co-evolution of behaviors and social relationships using mobile phone data," in *Proc. MUM*, 2011.
[56] Z. Wang, C. Xia, Z. Chen, and G. Chen, "Epidemic propagation with positive and negative preventive information in multiplex networks," *IEEE Trans. Cybern.*, vol. 51, no. 3, pp. 1454–1462, Mar. 2021.

Xianli Sun is currently pursuing the Ph.D. degree with the College of Telecommunications and Information Engineering, Nanjing University of Posts and Telecommunications (NJUPT). Her research interests include the theory of network control, optimization, and machine learning.

Linghua Zhang received the M.S. degree in Signal and Information Processing from Southeast University and the Ph.D. degree in Signal and Information Processing from the Nanjing Univer sity of Posts and Telecommunications, Nanjing, China, in 1990 and 2005, respectively, where she is currently a Professor and a Ph.D. Supervisor with the College of Telecommunications and Information Engineering. Her research interests include speech signal processing, voice communication, and signal processing in wireless communication.

Qiqing Zhai received the Ph.D. degree in Signal and Information processing from the Nanjing University of Posts and Telecommunications (NJUPT), Nanjing. His research interests include the theory of network control, optimization, and machine learning.

Peng Zheng is currently pursuing the Master degree with the College of Computer Science and Technology, Nanjing University of Posts and Telecommunications. His research focuses on satellite internet and communication technology.